System Identification for Human Motion Control

A frequency domain approach

Martijn P. Vlaar, Alfred C. Schouten
Department of BioMechanical Engineering
Delft University of Technology,
Delft, The Netherlands
m.p.vlaar@tudelft.nl

Alfred C. Schouten
Department of BioMechanical Engineering
University of Twente,
Enschede, The Netherlands

***Abstract*—System identification is an important tool to investigate human motion control. The goal of this study was to identify and address issues in system identification for human motor control and to investigate if linear time invariant system identification techniques are applicable to recorded mechanical and physiological data. During a posture maintenance experiment subjects had to minimize the deviations of the wrist, while a manipulator applied disturbances through a handle. We estimated frequency response functions and categorized and quantified the errors influencing the estimates. The relation between the position and force of the wrist was found to be highly linear and variations over time were the dominant source of error. The relation between the position changes at the wrist and the recorded signals from the brain was highly nonlinear. System identification techniques based on periodic multisine perturbation signals are a promising approach to investigate human motion control, even in the presence of inherent noise and nonlinearities.**

Keywords—Human motion control; sensory feedback; reflexes; best linear approximation; robotic manipulator; electromyography; electroencephalography

I. INTRODUCTION

Humans plan and execute complex movements, and have the ability to correct for disturbances while executing these movements. This feed forward and feedback control is facilitated by the central nervous system (controller) in conjunction with muscles (actuators) and proprioceptors (sensors). Malfunctioning of one of these components can lead to erroneous or no control, resulting in movement disorders such as tremor, Parkinsonism and dystonia. Movement disorders are among the most common neurological diseases in middle-aged and elderly people, having a prevalence of 28% for people over 50 years old [1]. Despite their commonness, proper diagnosis and subsequent treatment are still hampered because the pathophysiology of many movement disorders remains unclear, although disturbed sensory function or sensorimotor integration is often implicated [2]. An improved understanding of movement disorders can expedite diagnosis and improve treatment.

The research leading to these results has received funding from the European Research Council under the European Union's Seventh Framework Programme (FP/2007-2013) ERC Grant Agreement n. 291339, project 4D-EEG: A new tool to investigate the spatial and temporal activity patterns in the brain.

System identification is an emerging tool in biomechanics and human motion control and allows assessing system behavior in a quantitative way. However to unravel the functioning of human motion control we need techniques that can deal with specific requirements. Humans **are able to perform motions in numerous ways**, **interact** with their environment, **change their behavior** during an experiment, get **bored**, get **tired** and behave **nonlinear**. The goal of this study was to identify and address issues in system identification for human motor control and to investigate if linear time invariant system identification techniques are applicable to recorded mechanical and physiological data.

We first discuss the major challenges in studying human motion control and how these challenges can be addressed. Secondly we provide an experimental protocol to illustrate how these challenges influence the protocol, with a focus on the recent developments in frequency domain methods [3]. Third and finally we show and interpret experimental data and evaluate the quality of the data.

II. CHALLENGES

Humans can generate movements and forces in many ways due to the redundancy of the musculoskeletal system [4]. This redundancy can be mitigated by presenting a person with a clear unambiguous postural control task. Selecting a task which resembles a task in daily life allows for studying the execution of a functionally relevant task. During a postural control task, several signals can be recorded which all provide information on task execution: the position of and the force on the joint, electrical activity produced by the muscles controlling the joint (electromyogram, EMG) and by the brain (with for example electroencephalogram, EEG). The following section illustrates that presenting a person with a postural control task and the subsequent system identification is not straightforward.

A. Closed loop problem

Sensory feedback is crucial in human motion control, for example when a person is correcting for a disturbance which can be internal (e.g. spasms) or external (e.g. the movements when standing in a train). Since the person will be interacting with his environment, he will be operating in a closed loop in

which cause and effect are hard to distinguish. When studying sensory feedback it is therefore essential to provide a known external disturbance to a person and employ closed loop system identification techniques to open the loop [3].

B. Measurement setup and perturbation signal

To properly investigate a postural control task with external disturbance requires a robotic manipulator (see also Fig. 1). A range of robotic manipulators exist which allows for studying different limbs [5][6][7][8][9][10][11]. These robotic manipulators ensure well-conditioned experiments with high repeatability, and provide a quantitative way of assessing human postural control. When using a robotic manipulator perturbations can be presented as position or force perturbations. Several tasks can be performed using this measurement setup, amongst which a position task, force task and relax task (see Table I). In a position task subjects have to control the position of the limb (e.g. operating the gas pedal of a car), which is achieved by increasing the stiffness to oppose the perturbations. During a force task subjects have to control the force of the limb (e.g. minimizing force on the arm when walking with a cup of coffee), which is achieved by being compliant and thereby giving way to the perturbations. In a relax task subjects do not control the limb (i.e. relax) while perturbations are applied, allowing for assessment of the passive behavior. Healthy persons can adapt their mechanical admittance to the task at hand [5], where certain impaired individuals might not adapt properly [6]. Position tasks with force perturbations are more natural to the human, however require more advanced, more powerful and more expensive manipulators.

Humans have two main strategies which can be employed to perform postural control tasks: muscle co-contraction and sensory feedback. Muscle co-contraction requires antagonistic muscles to constantly activate and therewith increase stiffness without movement at the cost of high energy consumption. Sensors in the muscles and tendons can register position and force which allows for feedback control of the limb. Due to the time delay involved in signal transport via the neural pathways, sensory feedback can only be employed to the level where they do not cause instability of the limb. Humans adapt the use of their sensory feedback to the task at hand [5][12]. Unambiguous task instruction and extensive training prevent time variant adaptation of sensory feedback during an experiment.

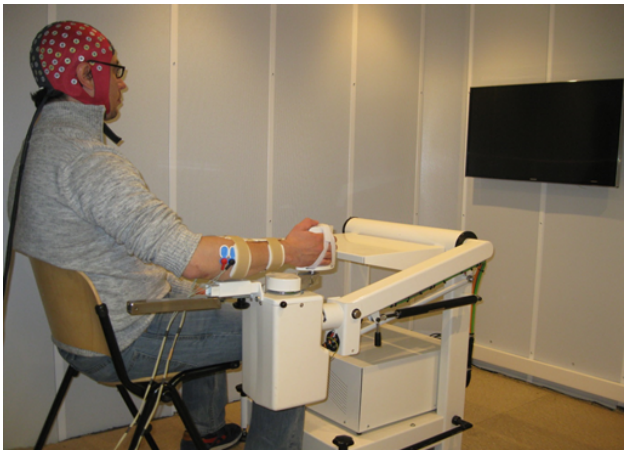

Fig. 1. Experimental setup. The right forearm of the subject is strapped into an armrest and the right hand is strapped to the handle, requiring no hand force to hold the handle. Both angle of and torque at the axis of the motor are recorded.

Many types of perturbation signals have been used in system identification for human motion control, including transients, white (or colored) noise, pseudo random binary sequences [13] and multisine signals [5][6][8]. A multisine signal is defined as:

$$r(t) = \sum_{k=1}^{N-1} A_k \cos\left(2\pi f_0 kt + \phi_k\right) \tag{1}$$

where k is the frequency line (integer number), A_k and ϕ_k are the amplitude and phase at frequency line k, f_0 is the frequency resolution in hertz, N is the number of samples in one period and t is the time vector describing one period of the signal. Frequency line k corresponds to the Fourier coefficients, where k=0 is the DC coefficient and is omitted to obtain a zero-mean signal. Multisine signals have several merits amongst which a customizable frequency content enabling increased signal-to-noise ratio (SNR) per frequency, leakage free analysis and the ability to detect and quantify nonlinear distortions [3].

In a position task the level to which the use of sensory feedback is effective depends on the contents of the perturbation signal, so when using multisine signals certain adaptation can be evoked by shaping the perturbation signal. When the perturbation signal contains power at higher frequencies, typically above the natural frequency of the limb the use of sensory feedback is hampered [14]. Perturbation signals with no power at the higher frequencies do not allow for identifying the systems response at higher frequencies. A solution is found in the reduced power method [15], where the bulk of the power is concentrated in the lower frequencies while there is still a portion of the power in the higher frequencies allowing system identification, albeit with low SNR.

When a multisine perturbation signal containing a low number of excited frequencies is applied many times in an experiment, the signal can become predictable, resulting in feed forward control. An unpredictable perturbation signal ensures feedback control.

To facilitate comparison between subjects, the excursions of the limb should be in a similar range over subjects. This can be accomplished by setting the intensity of the perturbation signal individually. Finding the proper intensity is typically done by trial and error, requiring additional time. Another option is to relate the intensity of the perturbations to the maximal voluntary contraction of the subject.

C. Nonlinear and time-varying behaviour

The sensors in the human body often behave nonlinearly [16] and the physiology of the muscle, which only allows it to contract, can also introduce nonlinear behavior [17]. In addition, the geometry of the limbs changes during a motion. Limiting the magnitude of the perturbations ensures study of the system in a small working range, which facilitates

TABLE I. EFFECT OF DIFFERENT PERTURBATION TYPES ON SUBJECT'S BEHAVIOR FOR DIFFERENT TASKS

Task type	Perturbation type	
	Position perturbations	***Force perturbations***
Position	Not feasible: subject will notice they have no influence on position	Feasible: subject will decrease their mechanical admittance
Force	Feasible: subject will increase their mechanical admittance	Feasible: subject will not notice he has no influence on force level. A virtual environment is required to prevent drift.
Relax	Feasible	Feasible: A virtual environment can be added to ensure the limb stays in the operating point.

linearization and thereby enables linear system identification techniques. Even though an attempt is made to linearize the system by keeping its working range small, certain strategies in task execution might cause nonlinear behavior. Humans tend to minimize their energy consumption, which could lead to intermittent control [5]. In intermittent control small errors are ignored and only when the error crosses a certain threshold action will be taken.

In the first few seconds of a postural control task, a subject is still adapting, causing a transient effect. Therefore the first seconds of every recording are disregarded.

Experiments involving posture control are often lengthy and monotonous, leading to inattention and boredom. Challenging tasks and social breaks are required to keep subjects motivated. Designing an appealing interface with a (serious) gaming character can aid in exciting subjects to perform well.

A limb can be attached to the robotic manipulator with fixation materials such as cast or Velcro straps, or the subject can keep hold of the robotic manipulator himself. In the former case it is important to balance comfort and quality of the coupling, whereas in the latter case grip can change over time due to sweaty, fatigued or sore hands.

Performing postural control tasks, specifically the position task, is strenuous for the muscles. Prolonged contraction of a muscle can lead to muscle fatigue, resulting in reduced muscle force. Muscle fatigue can be prevented by limiting the contraction time, where 30 to 40 seconds has proven to be a suitable experiment duration [5][8][11]. Having breaks in between trials gives muscles the change to recuperate and enables continuation of the experiment.

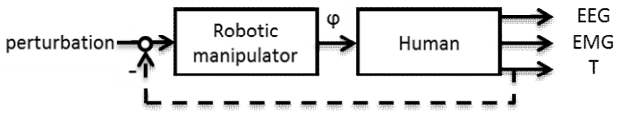

Fig. 2. Block scheme depicting the robotic manipulator and the human. The perturbation signal (position or torque) is passed on to the human by the robotic manipulator, which will impose a wrist angle (ϕ) on the human. In case of the torque perturbation (as is the case in this study) the torque on the handle (T) is fed back to the robotic manipulator (dashed line). The robotic manipulator ensures the angle is set such that the torque on the handle (T) matches the perturbation signal. Since in the case of torque perturbations the subject experiences an imposed torque (input) while he controls the angle (output), the mechanical behavior will be described as an admittance.

III. EXPERIMENT DESIGN

In this section we present the choices involved in a postural control experiment on the wrist to demonstrate how the challenges can be addressed. The goal of the experiment was to investigate if linear time invariant system identification techniques are applicable to mechanical, EMG and EEG data.

A. Experimental protocol

The experiments were performed on the wrist of the right arm, see Fig. 1. Subjects (N=11) were instructed to minimize the deviations of the handle (i.e., a position task) while torque perturbations were applied. The intensity of the perturbations was set such that all subjects had an rms wrist excursion of around 0.02 rad (≈1.1 deg). Handle angle and torque, applied perturbation signal, EMG and EEG were recorded at 2,048 Hz (Refa system by TMSi, Oldenzaal, The Netherlands), see Fig. 2. The EMG was recorded from the flexor and extensor carpi radialis. EMG signals were high-pass filtered using a fourth order Butterworth filter (cut-off frequency 25 Hz,) to reduce motion artifacts, and were subsequently rectified. The EEG was recorded from 128 channels, were only one channel close to the contralateral sensorimotor area was analyzed here.

B. Perturbation signal design

The following experiment design choices were made:

- The perturbation signal length was set to 1 second, which results in a frequency resolution of 1 Hz. This allows for a high number of repetitions in the same recording time, which is required for EEG due to its low SNR.
- Seven different multisine realizations are used, which have equal power distribution over the frequencies and yet each has a different random phase realization. The phases for each realization are taken from a uniform distribution (between 0 and 2π rad). The different phase realizations prevent prediction of the perturbation signal and allow quantification of the level of stochastic nonlinear distortions [3].
- The excited frequencies were: 1, 3, 5, 7, 9 ,11, 13, 15, 19, 23 Hz. Exciting only the odd frequencies allows for distinction between even and odd nonlinear distortions, and eliminates the disturbing effect of even distortions on the excited frequencies. Omitting 17, 21 and frequencies above 23 Hz limited the power in the high frequencies, which facilitates the use of sensory feedback. All excited frequencies contained equal power.
- Trials lasted 36 seconds and where designed by (smoothly) concatenating several periods of three different multisine realizations, which were randomly picked out of the seven generated multisine realizations.

This was done to prevent predictability of the signal at the cost of having to remove the periods containing the transitions between multisine realizations. Additionally the first recorded periods were removed from each trial to remove transient effects, resulting in three blocks of ten usable periods from each trial. A total of 49 trials was recorded leading to a total of 1470 recorded periods. This results in 210 periods for each of the seven realizations (M=7). These 210 periods are spread over trials in blocks of ten consecutively recorded periods (P=10), resulting in 21 blocks (Q=21) per realization.

- There was a minimal break of ten seconds between trials and there were several longer breaks to prevent fatigue.

C. Analysis

The analysis is largely based on the 'robust method' as described in [3]. Perturbing the system with several periods of the same multisine allows for estimation of the noise level. Perturbing the system with multisine signals which have a different phase distribution allows for estimation of the level of stochastic nonlinear distortions.

Turning phase of the recorded signals w.r.t. the perturbation signal (2) allows for averaging of the different realizations.

$$X_R^{[m,q,p]}(f) = \frac{X^{[m,q,p]}(f)}{e^{j\angle R^{[m]}(f)}} \tag{2}$$

Here $X^{[m,q,p]}(f)$ is a generic signal name for one of the Fourier transformed recorded signals, where the index m represents the realization (M=7), q the block (Q=21) and p the period (P=10). $R^{[m]}(f)$ is the Fourier transformed perturbation signal, which differs over realizations and not over blocks and periods. The frequency index (f) is omitted from the following equations for notational simplicity.

An estimate of the noise (co)variance is obtained by calculating the (co)variance over the periods (P) and averaging this estimate over all blocks (Q) and all realizations (M) (3).

$$\hat{\sigma}^2_{X_R Z_R,n} = \frac{1}{M}\sum_{m=1}^{M}\frac{1}{Q}\sum_{q=1}^{Q}\operatorname{cov}_p\left(X_R^{[m,q,p]}, Z_R^{[m,q,p]}\right) \tag{3}$$

Here X and Z can be the same or different recorded signals. An addition to the 'robust method' is the ability to quantify behavioral changes in between trials. A change in for example strategy, posture or handle grip will result in a different response to the perturbation signal irrespective of the multisine realization.

By estimating the variance over the averaged responses for each block (Q) per realization (M) (4) and averaging these estimates for all realizations (M), a variance is obtained which reflects noise and behavioral changes (5).

$$\hat{X}_R^{[m,q]} = \frac{1}{P}\sum_{p=1}^{P} X_R^{[m,q,p]} \tag{4}$$

$$\hat{\sigma}^2_{X_R Z_R,q} = \frac{1}{M}\sum_{m=1}^{M}\operatorname{cov}_q\left(X_R^{[m,q]}, Z_R^{[m,q]}\right) \tag{5}$$

The variance over the averaged responses for each realization (M) (6) reflects noise, behavioral changes, and stochastic nonlinear distortions (7).

$$\hat{X}_R^{[m]} = \frac{1}{Q}\sum_{q=1}^{Q} X_R^{[m,q]} \tag{6}$$

$$\hat{\sigma}^2_{X_R Z_R,m} = \operatorname{cov}\left(X_R^{[m]}, Z_R^{[m]}\right) \tag{7}$$

The final averaged response for each recorded signal is obtained in (8).

$$\hat{X}_R = \frac{1}{M}\sum_{m=1}^{M} X_R^{[m]} \tag{8}$$

The transfer function between an input (U) and output (Y) of the system is obtained by substituting X and Z in (1-7) by U and/or Y and by estimating the best linear approximation (9). For the mechanical admittance the input is force and output is angle. For reflexive impedance the input is angle and the output is EMG. The transfer function regarding the recorded EEG is defined using the recorded wrist angle as input and the recorded EEG as output.

$$\hat{G}_{BLA} = \frac{\hat{Y}_R}{\hat{U}_R} \tag{9}$$

Uncertainties on this transfer function can now be distinguished in $\hat{\sigma}^2_{G,n}(f)$, $\hat{\sigma}^2_{G,q}(f)$ and $\hat{\sigma}^2_{G,m}(f)$, by inserting the result of (3), (5) or (7) in (10) where the asterisk is replaced by either n, q, or m.

$$\hat{\sigma}^2_{G,*} = \left|\hat{G}_{BLA}\right|^2\left(\frac{\hat{\sigma}^2_{Y_R,*}}{\left|\hat{Y}_R\right|} + \frac{\hat{\sigma}^2_{U_R,*}}{\left|\hat{U}_R\right|} - 2\operatorname{Re}\left(\frac{\hat{\sigma}^2_{Y_R U_R,*}}{\hat{Y}_R\overline{\hat{U}_R}}\right)\right) \tag{10}$$

The errors on the final estimate of $\hat{G}_{BLA}$ due to noise will converge to zero as M, Q and P tend to infinity. The errors on the final estimate of $\hat{G}_{BLA}$ due to stochastic nonlinear distortions will converge to zero as M tends to infinity. The effect of errors due to behavioral changes between trials on the final estimate of $\hat{G}_{BLA}$ is less clear. Here we will assume these errors will converge to zero as M and Q tend to infinity. It is expected these errors arise from slight changes in posture and handle grip in between trials and after breaks. A slow drift in behavior due to (muscle) fatigue, change in strategy and boredom also contribute to errors due to behavioral changes, however should be minimal due to extensive training and breaks. It is likely that these slow drifts would also result in reduced performance over time, which was not observed in this experiment. If the assumption on convergence is too strong, the error due to behavioral changes will be underestimated and consequently the errors due to stochastic nonlinear distortions will be overestimated. The errors remaining in the final

estimate $\hat{G}_{BLA}$ are presented as sample standard deviations in (11).

$$\begin{aligned}\hat{\sigma}_{G,n,err} &= \sqrt{\frac{1}{MQP}\hat{\sigma}^2_{G,n}} \\ \hat{\sigma}_{G,q,err} &= \sqrt{\frac{1}{MQ}\hat{\sigma}^2_{G,q}} \\ \hat{\sigma}_{G,m,err} &= \sqrt{\frac{1}{M}\hat{\sigma}^2_{G,m}}\end{aligned} \tag{11}$$

The errors on $\hat{G}_{BLA}$ w.r.t. one recording block (Q) caused by behavioral changes ($\hat{\sigma}_{G,BC}$) are obtained using (12). Here $\hat{\sigma}_{G,BC}$ is presented as standard deviation, where the noise level $\hat{\sigma}^2_{G,n}$ is scaled by 1/P to reflect the noise level in $\hat{\sigma}^2_{G,q}$ after averaging.

$$\hat{\sigma}_{G,BC} = \begin{cases} \sqrt{\hat{\sigma}^2_{G,q} - \frac{1}{P}\hat{\sigma}^2_{G,n}} & \hat{\sigma}^2_{G,q}(f) > \frac{1}{P}\hat{\sigma}^2_{G,n}(f) \\ 0 & \hat{\sigma}^2_{G,q}(f) \le \frac{1}{P}\hat{\sigma}^2_{G,n}(f) \end{cases} \tag{12}$$

The standard deviation due to stochastic nonlinear distortions ($\hat{\sigma}_{G,SNL}$) w.r.t. one realization (M) is obtained using (13), where $\hat{\sigma}^2_{G,q}$ is scaled by 1/Q to reflect the level of behavioral changes and noise in $\hat{\sigma}^2_{G,m}$ after averaging.

$$\hat{\sigma}_{G,SNL} = \begin{cases} \sqrt{\hat{\sigma}^2_{G,m} - \frac{1}{Q}\hat{\sigma}^2_{G,q}} & \hat{\sigma}^2_{G,m}(f) > \frac{1}{Q}\hat{\sigma}^2_{G,q}(f) \\ 0 & \hat{\sigma}^2_{G,m}(f) \le \frac{1}{Q}\hat{\sigma}^2_{G,q}(f) \end{cases} \tag{13}$$

Slow time variant behavior within each block (Q) of ten consecutively recorded periods (P) can be detected with methods described in [18]. Checking the power at the even and unexcited odd frequency lines enables distinction between even and odd nonlinear systems, which can aid the selection process in a possible nonlinear modelling step.

IV. Experiment Results

A. Best Linear Approximation

Fig. 3 shows the mechanical admittance, reflexive impedance and transfer function from angle to EEG for a typical subject. In the mechanical admittance plot behavioral changes are the dominant source of variance on the BLA, which in the normal robust method would erroneously be attributed to stochastic nonlinear distortions. The reflexive impedance plot for the flexor muscle shows, compared to the mechanical admittance plot, more stochastic nonlinear distortions. The extensor muscle shows similar behavior (results not shown). In the relation between angle and EEG the stochastic nonlinear distortions are at the level of the BLA, indicating a highly nonlinear response.

B. Interpretation

In the mechanical admittance plot, the low frequencies represent the combined stiffness of intrinsic and reflexive contributions. The increased variance levels around the natural frequency of the limb are to be expected, since the natural frequency shifts due to the small variations in stiffness of the limb. This stiffness can change due to for example change in strategy, fatigue and change in contact dynamics. The response at the high frequencies is mainly governed by the inertia of the limb. In this frequency region the level of behavioral changes drops, since the subject has little influence on response. There is however still an indication of stochastic nonlinear distortions, indicating that the mechanical admittance cannot be

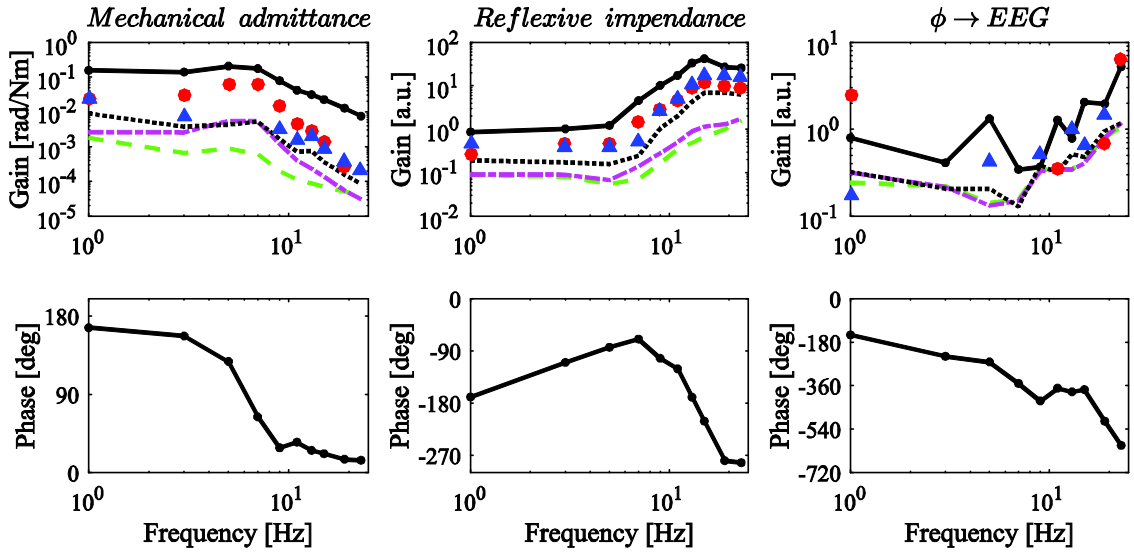

Fig. 3. Three frequency response functions (FRF) for a typical subject: mechanical admittance, reflexive impedance (flexor muscle) and from angle to EEG. Solid black line indicates the BLA (gain and phase), dotted black lines give the total sample standard deviation on the estimated BLA, dash-dotted magenta line gives the sample standard deviation due to noise and behavioral changes, dashed green line gives the sample standard deviation due to noise. Blue triangles and red circles give the level of stochastic nonlinear distortions w.r.t to one realization M and behavorial changes w.r.t. one block (Q) respectively.

fully described by a linear model. The bump around 10 Hz, which is most evident in the phase plot, is assumed to be caused by contact dynamics between the limb and the robotic manipulator.

The reflexive impedance plot shows the system behaves as a PD controller. The decline in the phase indicates the neural time delay associated with sensory feedback. The stochastic nonlinear distortions can partly be explained by the physiology of a muscle which only allows it to actively shorten and not extend, making it behave like a half wave rectifier.

The transfer function from angle to EEG does not allow for much interpretation beyond the observation the relation is besides noisy, highly nonlinear. An analysis on the power per frequency indicates the bulk of the power is concentrated in the unexcited frequencies. This indicates that a linear time invariant (LTI) approach will not suffice to study the EEG response.

V. Conclusions

System identification is an important tool to investigate and better understand the dynamics of the human neuromuscular system, which is crucial to unravel the physiology of movement disorders. Novel frequency domain methods allow estimation of the best linear approximation (BLA) in the form of a frequency response function (FRF). Directly from the BLA, conclusions on human motion control can be drawn. The extra information accompanying the BLA allows for distinction between error sources. This facilitates validation of recorded data during analysis, yet also enables improvement of experimental paradigms. The "robust method" provides the BLA, an estimate of the noise and an estimate of the level of stochastic nonlinear distortions. The addition to the "robust method" allows checking for changes in behavior between trials caused by for example fatigue or change of strategy. It is crucial to check for time varying behavior and nonlinear distortions to see if an LTI approach is valid. For the mechanical admittance and reflexive impedance an LTI approach seems to be justified, yet the relation between the angle and the recorded EEG appears to be highly nonlinear and other approaches need to be explored.

These frequency domain techniques allowing for the indubitable importance of the validation of the recorded data are facilitated by the use of multisine signals and come at only a small expense and some considered decisions in the experiment design.

Acknowledgment

The authors would like to thank the members of the ELEC department of the Vrije Universiteit Brussel for their helpful discussions.

References

[1] G.K. Wenning et al., "Prevalence of movement disorders in men and women aged 50–89 years (Bruneck Study cohort): a population-based study," The Lancet Neurology, Volume 4, Issue 12, pp. 815-820, December 2005

[2] N. Patel, J. Jankovic and M. Hallett, "Sensory aspects of movement disorders," The Lancet Neurology, vol. 13, issue 1, pp. 100-112, 2014

[3] R. Pintelon and J. Schoukens, System identification: a frequency domain approach. John Wiley & Sons, 2012.

[4] D.W. Franklin and D.M. Wolpert, "Computational mechanisms of sensorimotor control," Neuron, vol. 72, issue 3, pp. 425-442, 2011

[5] W. Mugge, D.A. Abbink, A.C. Schouten, J.P.A. Dewald and F.C.T. van der Helm, "A rigorous model of reflex function indicates that position and force feedback are flexibly tuned to position and force tasks," Experimental brain research, vol. 200, issue 3-4, pp. 325-340, 2010

[6] C.G.M. Meskers et al., "Muscle weakness and lack of reflex gain adaptation predominate during post-stroke posture control of the wrist," Journal of neuroengineering and rehabilitation, vol. 6, issue 1, pp. 29, 2009

[7] E. de Vlugt, A.C. Schouten, F.C.T. van der Helm, P.C. Teerhuis and G.G. Brouwn, "A force-controlled planar haptic device for movement control analysis of the human arm," Journal of Neuroscience Methods, vol. 129, issue 2, pp. 151-168, October 2003

[8] A.C. Schouten, E. de Vlugt, J.J.B. van Hilten and F.C.T. van der Helm. "Quantifying proprioceptive reflexes during position control of the human arm," IEEE Transactions on Biomedical Engineering, vol. 55, no. 1, pp. 311-321, January 2008

[9] G.N. Lewis, C.D. MacKinnon, R. Trumbower, and E.J. Perreault. "Co-contraction modifies the stretch reflex elicited in muscles shortened by a joint perturbation," Experimental brain research, vol. 207, issue 1-2, pp 39-48, 2010

[10] D. Ludvig, I. Cathers and R.E. Kearney, "Voluntary modulation of human stretch reflexes," Experimental brain research, vol. 183, issue 2, pp 201-213, 2007

[11] M.M. Mirbagheri, H. Barbeau, and R.E. Kearney, R, "Intrinsic and reflex contributions to human ankle stiffness: variation with activation level and position," Experimental Brain Research, vol. 135, issue 4, pp 423-436, 2000

[12] A.C. Schouten, W. Mugge and F.C.T. van der Helm, "NMClab, a model to assess the contributions of muscle visco-elasticity and afferent feedback to joint dynamics," Journal of biomechanics, vol. 41, issue 8, pp. 1659-1667, 2008

[13] R.E. Kearney, R.B. Stein and L. Parameswaran, "Identification of intrinsic and reflex contributions to human ankle stiffness dynamics," IEEE Transactions on Biomedical Engineering, vol. 44, issue 6, pp. 493-504, 1997

[14] E. de Vlugt, A.C. Schouten and F.C.T. van der Helm, "Adaptation of reflexive feedback during arm posture to different environments," Biological cybernetics, vol. 87, issue 1, pp. 10-26, 2002

[15] W. Mugge, D.A. Abbink and F. C. T. Van der Helm, "Reduced power method: how to evoke low-bandwidth behaviour while estimating full-bandwidth dynamics," IEEE 10th International Conference on Rehabilitation Robotics, 2007

[16] M.P. Mileusnic, I.E. Brown, N. Lan and G.E. Loeb, "Mathematical models of proprioceptors. I. Control and transduction in the muscle spindle," Journal of neurophysiology, vol. 96, issue 4, pp. 1772-1788, 2006

[17] R.E. Kearney and I.W. Hunter, "Nonlinear identification of stretch reflex dynamics," Annals of biomedical engineering, vol. 16, issue 1, pp 79-94, 1988

[18] J. Lataire and R. Pintelon, "Estimating a Nonparametric Colored-Noise Model for Linear Slowly Time-Varying Systems," IEEE Transactions on Instrumentation and Measurement, vol. 58, issue 5, pp. 1535-1545, 2009